Supporting information

CuO-C modified glass fiber films with Mixed Ion and Electron-Conducting scaffold for highly stable Lithium Metal Anodes

Xiaojie Shen, [a] Guangyu Zhao, *[b] Lishuang Fan, [ab] Zhikun Guo, [a] Chenyang Zhao, [a] Aosai Chen, [a] Guiye Yang, [a] Zhongjun Cheng [a] and Naiqing Zhang *[ab]

a. State Key Laboratory of Urban Water Resource and Environment, School of Chemistry and Chemical Engineering, Harbin Institute of Technology, China.

b. Academy of Fundamental and Interdisciplinary Sciences, Harbin Institute of Technology, Harbin, 150001, China. Email: zhaogy810525@gmail.com; znqmww@163.com

Supplementary Figures

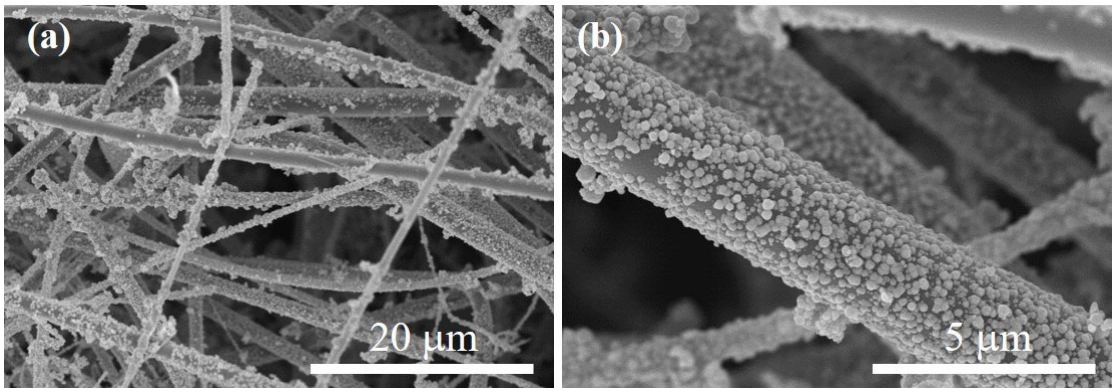

Figure S1. Morphologies of Cu-GFs fabricated by electroless plating copper on GFs (a) low and (b) high magnification.

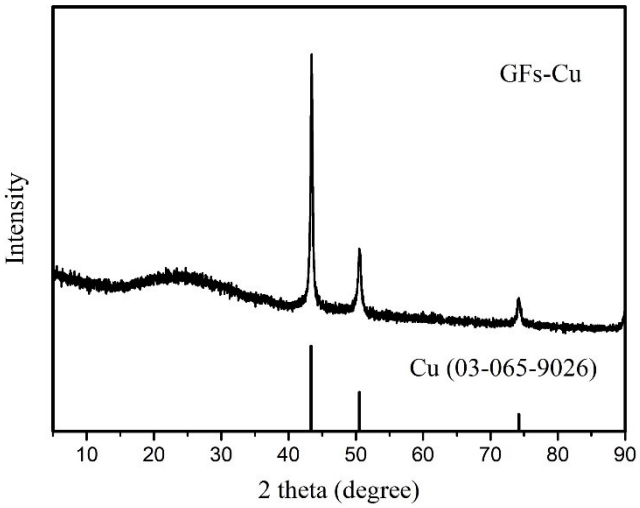

Figure S2. XRD patterns of Cu-GFs.

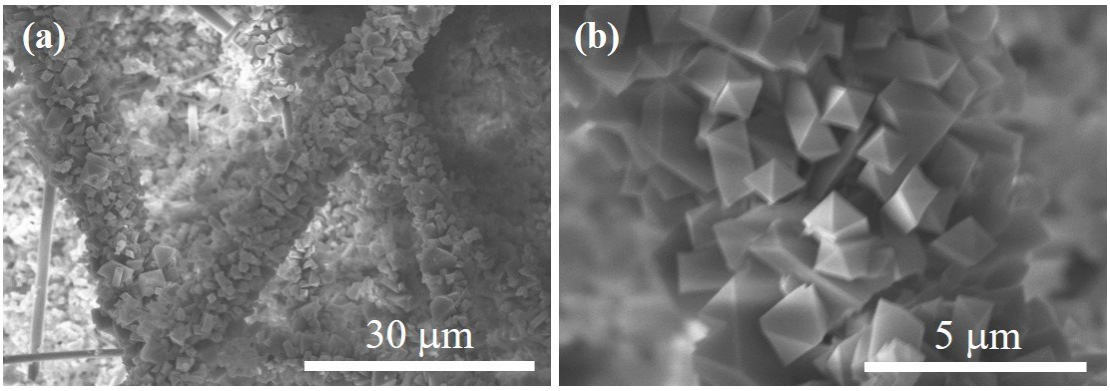

Figure S3. Morphologies of Cu-BTC-GFs (a) low and (b) high magnification.

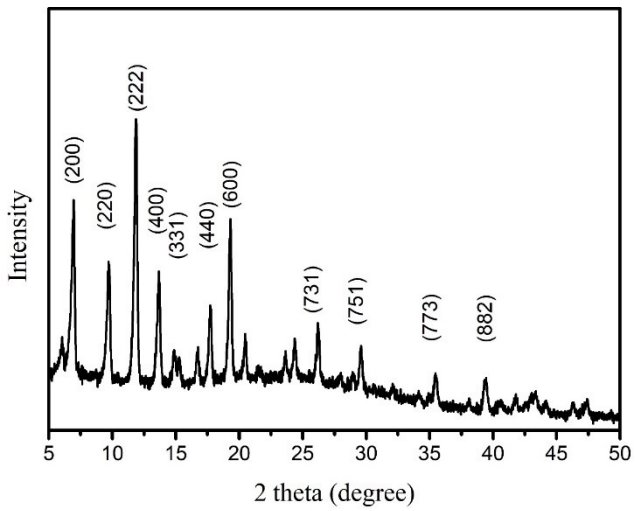

Figure S4. XRD patterns of Cu-BTC-GFs.

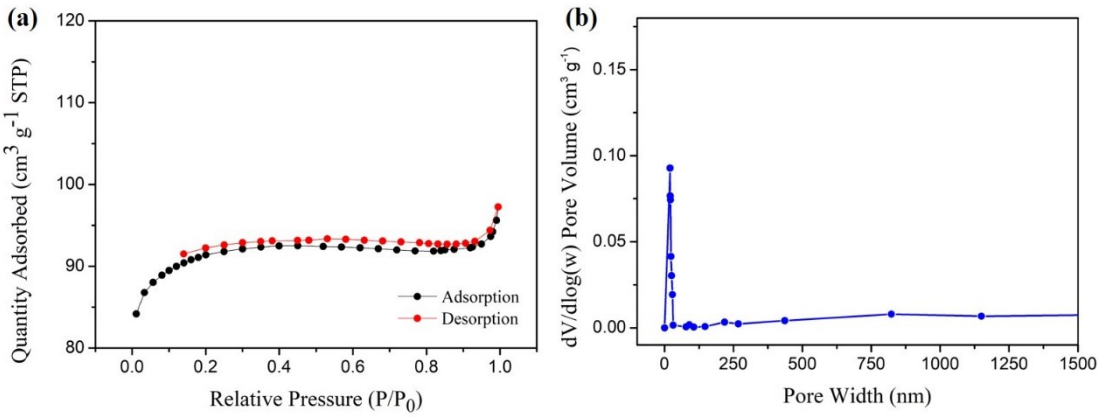

Figure S5. (a) Nitrogen adsorption/desorption isotherms of the Cu-BTC-GFs (b) pore-size distribution of the Cu-BTC-GFs.

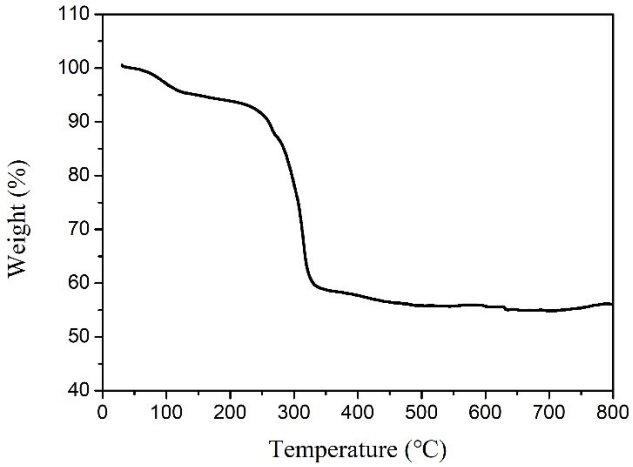

Figure S6. Thermogravimetric Analysis curves of the Cu-BTC-GFs in nitrogen flow.

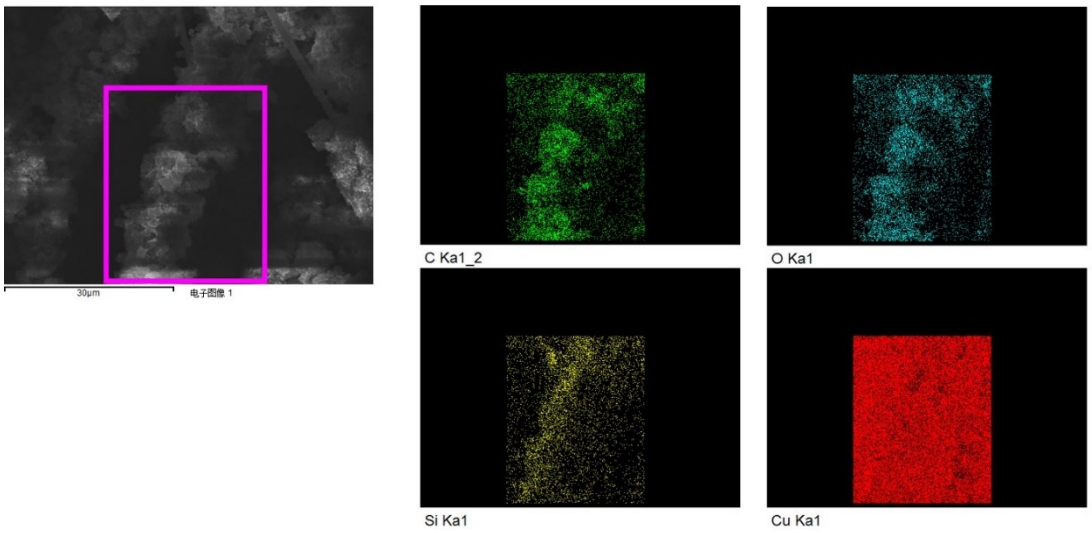

Figure S7. EDS diagram of CuO-C/MGFs.

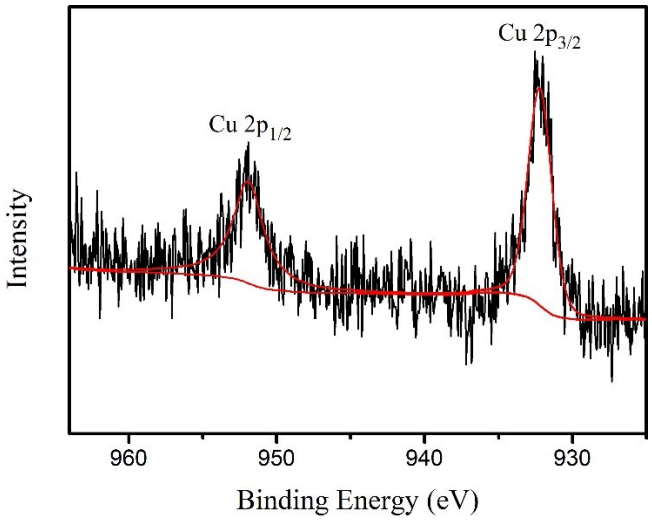

Figure S8. XPS spectra of Cu_{2p} spectra of Cu-C/MGFs.

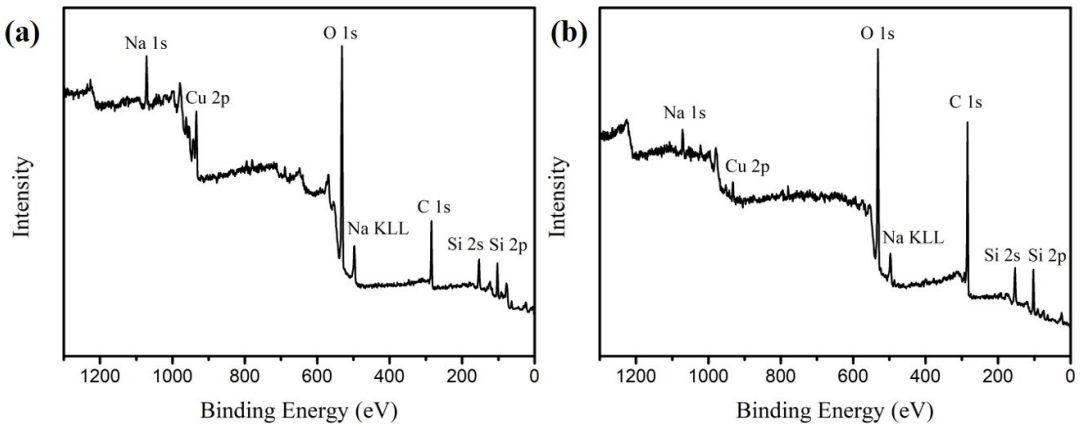

Figure S9. The survey of XPS spectra (a) CuO-C/MGFs (b) Cu-C/MGFs.

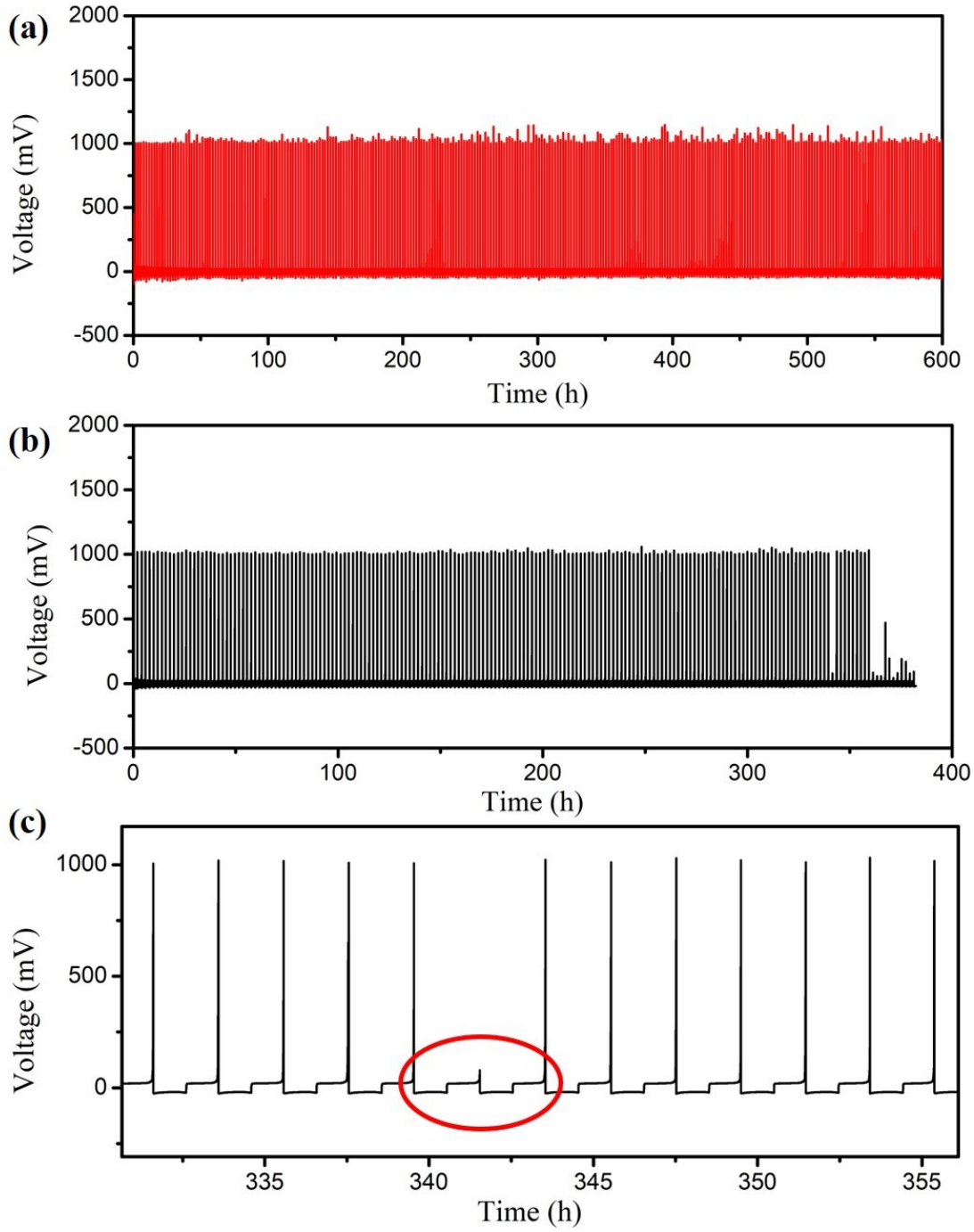

Figure S10. Galvanostatic charge and discharge curve during Coulomb efficiency test of (a) CuO-C/MGFs (b) Cu-C/MGFs (c) enlarged image of Cu-C/MGFs.

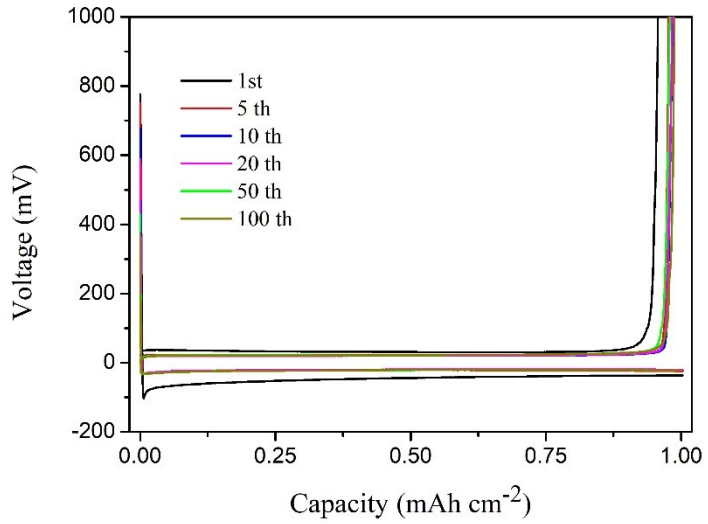

Figure S11. Voltage profiles with different cycles of lithium plated/stripped on Cu-C/MGFs at a current density of 1 mA cm^{-2} with a capacity of 1 mAh cm^{-2}.

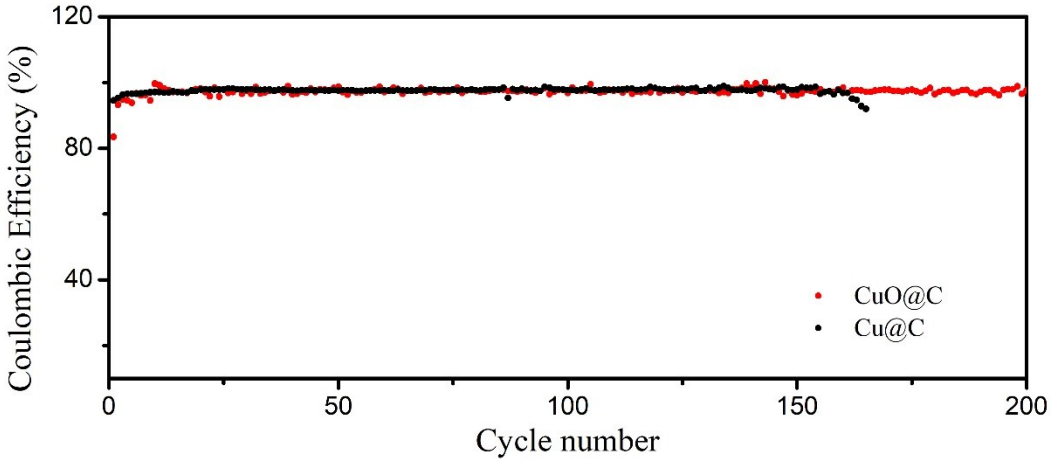

Figure S12. Coulombic efficiency of lithium plated on CuO-C/MGFs and Cu-C/MGFs with a mount of 1 mAh cm^{-2} at 2 mA cm^{-2}.

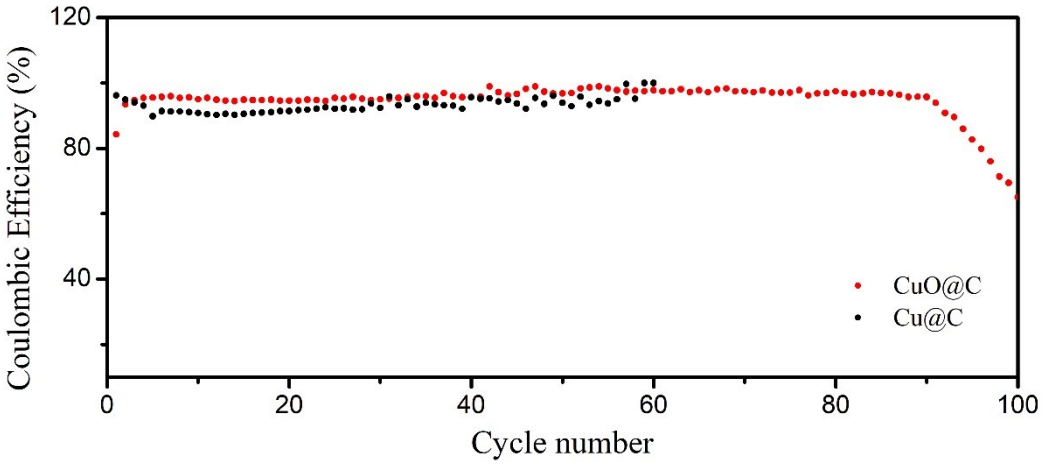

Figure S13. Coulombic efficiency of lithium plated on CuO-C/MGFs and Cu-C/MGFs with a mount of 1 mAh cm^{-2} at 5 mA cm^{-2}.

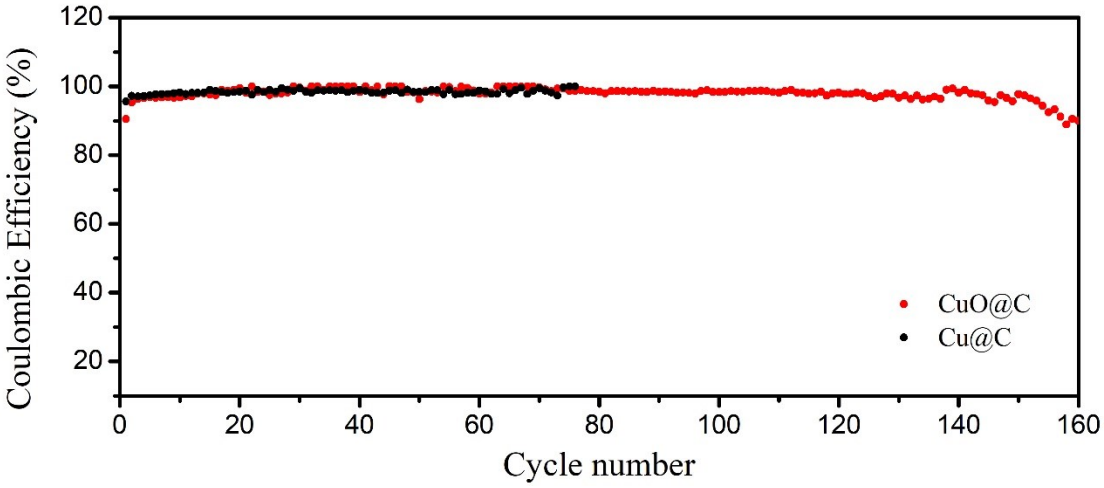

Figure S14. Coulombic efficiency of lithium plated on CuO-C/MGFs and Cu-C/MGFs with a mount of 2 mAh cm^{-2} at 1 mA cm^{-2}.

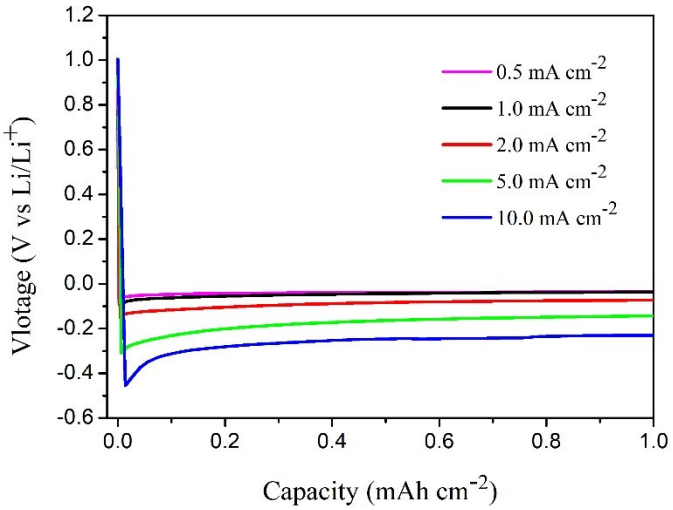

Figure S15. Voltage profiles of lithium plated on Cu-C/MGFs at different current densities with a capacity of 1mAh cm^{-2}.

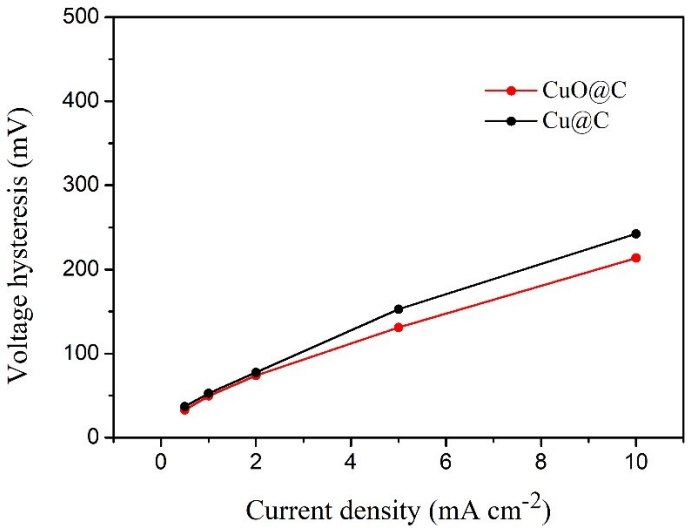

Figure S16. The lithium deposition voltage hysteresis of CuO-C/MGFs and Cu-C/MGFs at different current densities.

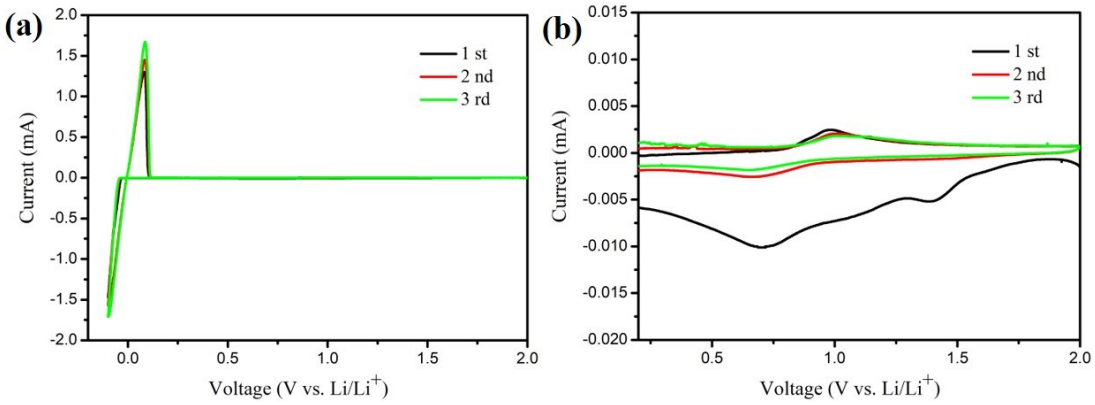

Figure S17. CV curves of CuO-C/MGFs anode countering to a lithium metal plate. Test voltage range is from 2.0 V to -0.1 V and the sweep speed is 0.1 mV s^{-1}.

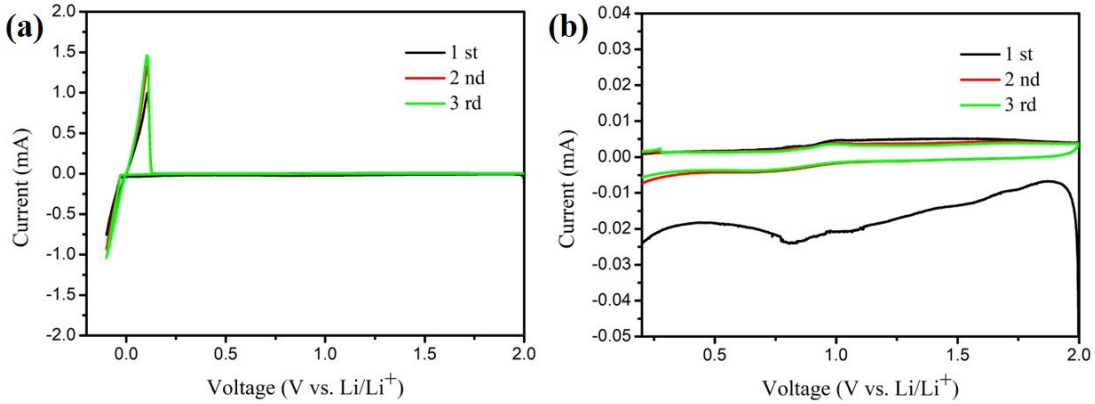

Figure S18. CV curves of Cu-C/MGFs anode countering to a lithium metal plate. Test voltage range is from 2.0 V to -0.1 V and the sweep speed is 0.1 mV s^{-1}.

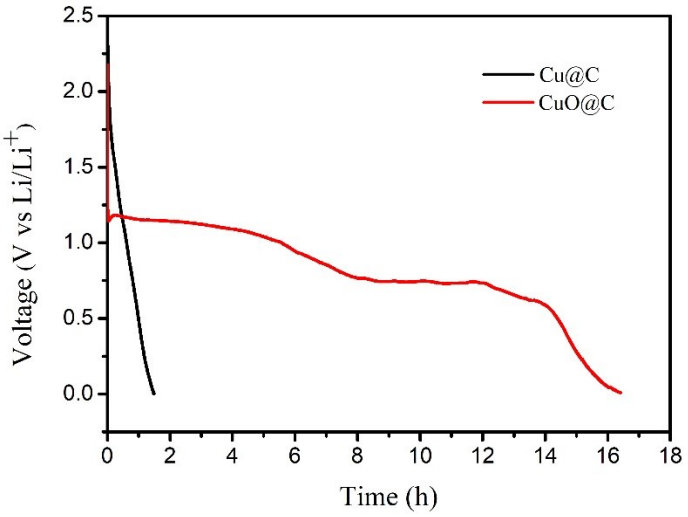

Figure S19. Voltage–time curve of CuO-C/MGFs and Cu-C/MGFs at 0.05 mA cm^{-2}.

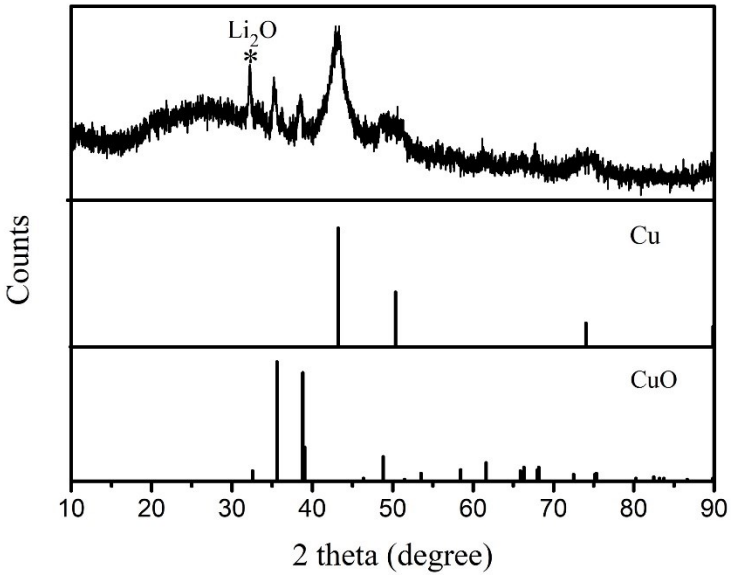

Figure S20. XRD patterns of CuO-C/MGFs anode after the first discharge.

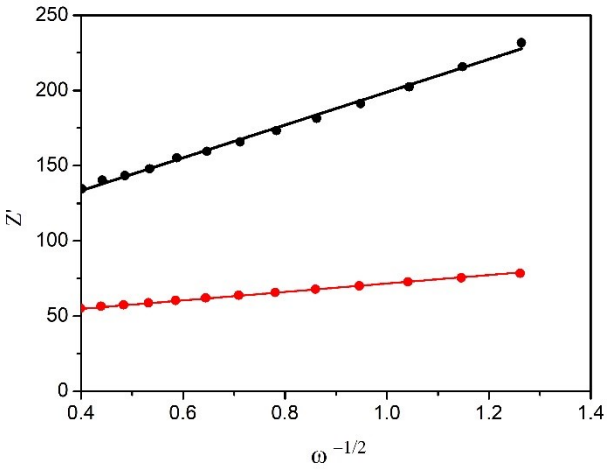

Figure S21. The fitted lines of the impedance versus $\omega^{-1/2}$ for CuO-C/MGFs anode (red) and Cu-C/MGFs anode (black).

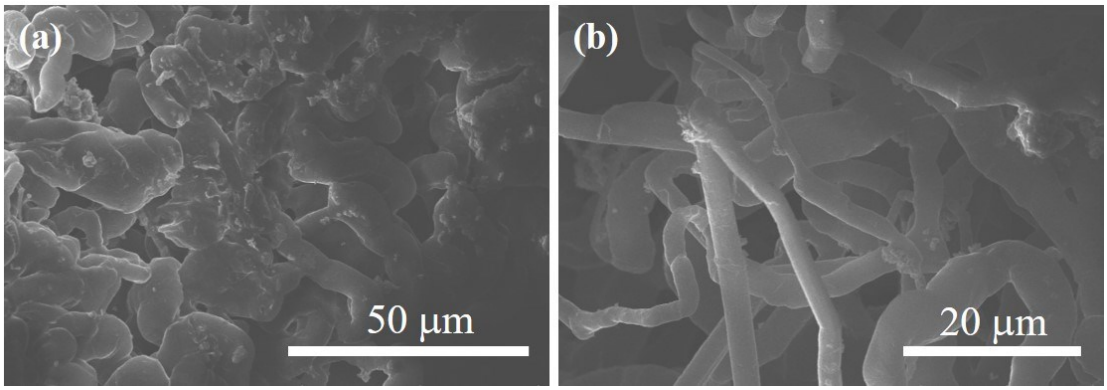

Figure S22. Morphologies of Cu-C/MGFs after deposited lithium in amount of 10 mAh cm^{-2} at a current density of 1 mA cm^{-2}.

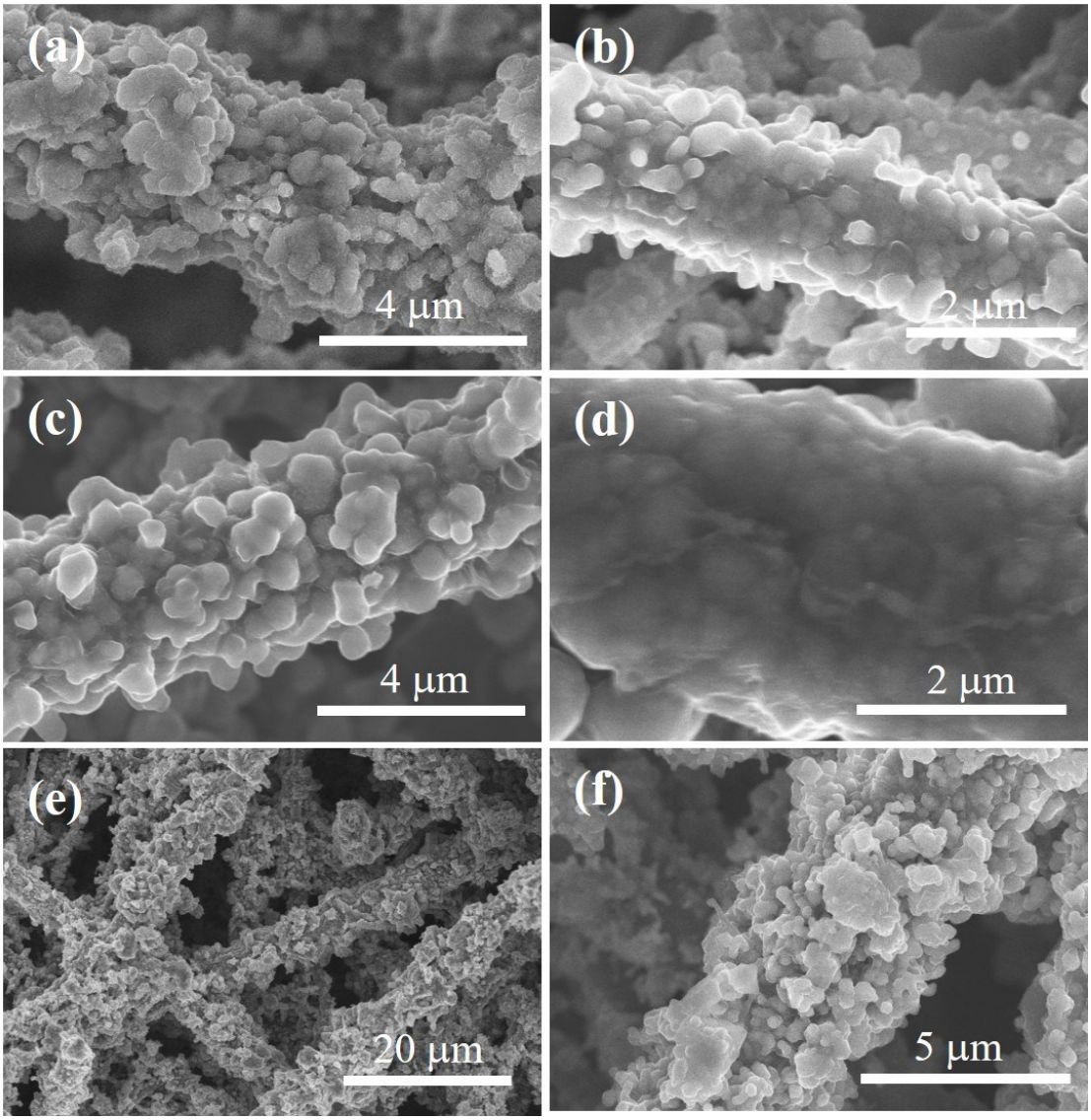

Figure S23. SEM images of the morphologies of lithium deposited on CuO-C/MGFs at a current density of 1mA cm^{-2} with the capacity of (a) 0.2 mAh cm^{-2} (b) 0.5 mAh cm^{-2} (c) 1 mAh cm^{-2} (d) 2 mAh cm^{-2} (e-f) lithium was totally stripped.

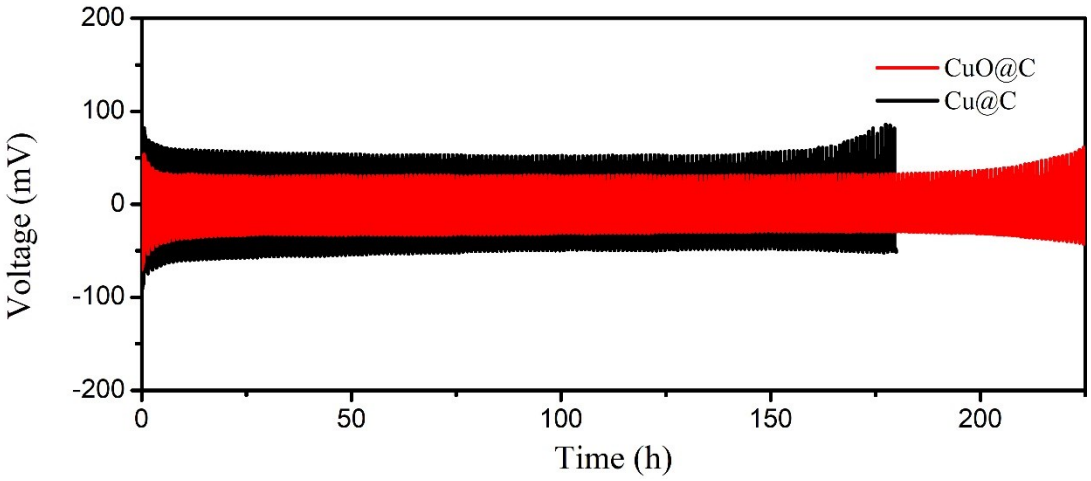

Figure S24. Voltage-time profiles of symmetric Li| Li/ CuO-C and Li| Li/ Cu-C batteries with a capacity of 1 mAh cm^{-2} Li at 2 mA cm^{-2}.

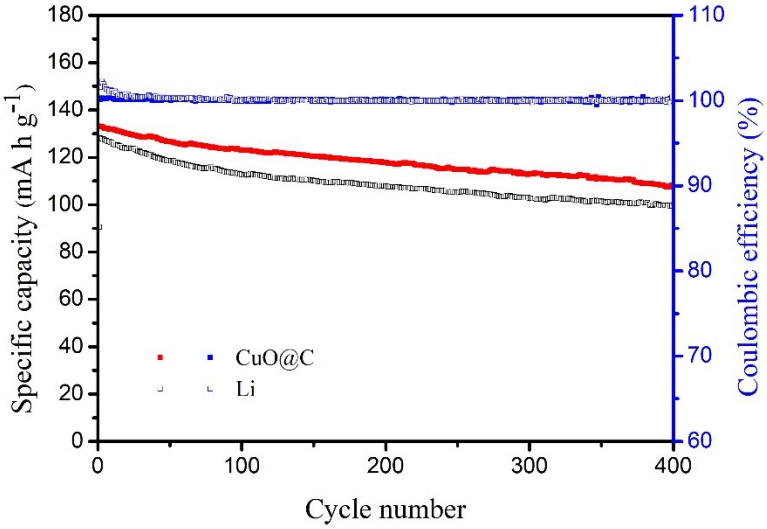

Figure S25. Cycling stability comparison of the full cells with CuO-C/MGFs anode and Li anode.

Table 1. Coulombic efficiency of CuO-C/MGFs compared with various anode substrates.

substrates	Current/ Capacity ($mA\ cm^{-2}$/ $mAh\ cm^{-2}$)	CE (%)	cycle	Max current ($mA\ cm^{-2}$)	Ref.
PDA@3D Cu	0.5/1	97.3	200	1	*Energy Storage Materials*, 2020, 29, 84-91
3D porous Cu current collector	1/1	97	140	1	*Adv. Mater.* 2016, 28, 6932-6939.
3D PI-clad copper	0.5/1	90	150	2	*Nat. Commun.* 2018, 9, 464.
g-C_3N_4@ Ni foam	2/1	97	140	3	*Adv. Energy Mater.* 2019, 9, 1803186.
3D porous Cu	1/1	97.9	200	1	*Adv. Energy Mater.* 2018, 8, 1800266
3D Cu@Al@Li	0.5/2	98.6	85	2	*Angew. Chem., Int. Ed.* 2019, 58, 1094-1099.
3D copper nanowire-phosphide	1/1	97.4	150	3	*Adv. Mater.* 2019, 31, 1904991
This work	1/1	98.1	400	5	
	5/1	96.2	90		